International Journal of Pharmaceutical Research and Applications
Volume 10, Issue 4 July-Aug 2025, pp: 934-948 www.ijprajournal.com ISSN: 2456-4494

"Development and Doe-Based Optimization of a Microencapsulated Crisaborole Drug Delivery System"

Babbu Singh Gurjar[1], Dharmendra Singh Rajput[2]*, Naveen Gupta[3]
[1]*Student- Patel College of Pharmacy (MPU), Bhopal, Madhya Pradesh*
[2]*Head of Department- Patel College of Pharmacy (MPU), Bhopal, Madhya Pradesh*
[3]*Dean- Patel College of Pharmacy (MPU), Bhopal, Madhya Pradesh*

Date of Submission: 15-08-2025 Date of Acceptance: 25-08-2025

ABSTRACT
The formulation of microcapsule containing crisaborole by Design of experiment. Microencapsulation, a widely adopted technique, enables the controlled release of active pharmaceutical ingredients (APIs) by encapsulating them in a protective polymer matrix. Microcapsules spherical shape and smooth surface morphology were demonstrated by a scanning electron micrograph with a magnification of 150.59 KX. The entrapment efficacy of produced optimized Microcapsules was found to have a high drug entrapment efficiency of 93.78%. The melting point (131°C) fell within the reference range, confirming purity and the absence of significant impurities. The pH of the drug sample (5.3) lies within the acceptable dermal application range, supporting its compatibility with skin physiology and reducing the risk of irritation. The solubility study showed that Crisaborole is highly soluble in methanol, moderately soluble in ethanol and acetone, but practically insoluble in water, indicating the need for specialized delivery systems. The UV spectroscopic analysis determined the λ max at 250 nm, and a linear calibration curve was established between 2–12 µg/mL concentrations. The high % RSD value (49.746%) suggests the need for improved analytical precision in future studies. FTIR analysis confirmed the structural integrity and compatibility of the drug in formulations. Overall, the results validate Crisaborole's potential as a candidate for stable, effective topical formulations and as a drug encapsulated in polymeric Microcapsules to improve its solubility and therapeutic efficacy. The research concludes that the application of DOE in Microcapsules formulation allows for a systematic and efficient approach to developing optimized nanocarriers for various applications.

Keywords: Sustained-release, microencapsulation, Crisaborole, Entrapment efficacy, Design of experiment

I. INTRODUCTION

Microencapsulation technologies such as spray drying, coacervation, solvent evaporation, and electrostatic coating have been widely adopted in this context due to their versatility and efficiency in controlling drug release profiles. The process involves atomizing a solution of the drug and polymer into fine droplets, which are quickly dried by a stream of hot air, forming microcapsules with controlled size and drug distribution **(Deshmukh et al., 2016).** This method is especially beneficial for drugs that are heat-sensitive, as the drying conditions can be carefully controlled to prevent degradation. Solvent evaporation, another common technique, enables the formation of uniform microspheres by dissolving the drug and polymer in a volatile organic solvent that gradually evaporates, leaving behind encapsulated particles. This method offers precise control over particle size and drug release kinetics, making it ideal for formulations requiring a high degree of release control **(Subedi et al., 2016).**

Sustained-release drug formulations have become a cornerstone in the treatment of chronic conditions, where maintaining a stable therapeutic level of drugs in the bloodstream is essential for effective disease management. Diseases like cardiovascular disorders, diabetes, and asthma require long-term medication, and sustained-release systems help to reduce the frequency of drug administration, thereby improving patient adherence and convenience **(Islam Barbhuiya et al., 2023).** The encapsulation technique used in formulating sustained-release drugs is crucial in determining the efficacy of the drug release profile. Among the various methods, spray drying, coacervation, solvent evaporation, and electrostatic coating have shown promise for their ability to produce microparticles that encapsulate APIs **(Natarajan et al., 2014).**

Crisaborole has broad-spectrum anti-inflammatory activity by mainly targeting phosphodiesterase 4 (PDE4) enzymes that is a key

International Journal of Pharmaceutical Research and Applications
Volume 10, Issue 4 July-Aug 2025, pp: 934-948 www.ijprajournal.com ISSN: 2456-4494

regulator of inflammatory cytokine production. As this enzyme is expressed in keratinocytes and immune cells, crisaborole mediates an anti-inflammatory effect on almost all inflammatory cells. Inhibition of PDE4 by crisaborole leads to elevated levels of cyclic adenosine monophosphate (cAMP) **(Li et al., 2018).** Increased intracellular levels of cAMP inhibit the NF-kB pathway and suppress the release of pro-inflammatory mediators such as TNF-alfa and various interleukins that play a causative role in psoriasis and atopic dermatitis. Suppression of downstream effects in different cell types may explain the therapeutic role of crisaborole in immune-mediated skin diseases. Crisaborole is substantially metabolized into inactive metabolites. The major metabolite 5-(4-cyanophenoxy)-2-hydroxyl benzylalcohol (metabolite 1), is formed via hydrolysis; this metabolite is further metabolized into downstream metabolites, among which 5-(4-cyanophenoxy)-2-hydroxyl benzoic acid (metabolite 2), formed via oxidation, is also a major metabolite **(McDowell and Olin 2019).**

The current study aims to formulate, developed and optimized the Microcapsule containing crisaborole by Design of experiment approach

II. MATERIALS AND METHODS

2.1 Chemicals

Ethanol, Acetonitrile, Propylene glycol and Methyl paraben were obtained from Merck. Sigma-Aldrlch provided the Crisaborole, Ethyl cellulose and PVA. Rankem provided the Methanol while Loba supplied Triethanolamine. Carbopol 934 was supplied by Sulab.

2.2 Pre-formulation studies

Pre-formulation studies of Crisaborole involve evaluating its physical and chemical properties to guide the development of a stable and effective dosage form. These studies include tests for solubility, stability, pH, melting point, and compatibility with excipients. They are performed using techniques like differential FTIR, UV spectroscopy, and other parameters to ensure the drug's suitability for formulation **(Vilegave et al., 2013).**

2.2.1 Organoleptic Properties

The organoleptic properties of Crisaborole refer to its sensory characteristics, such as color, odor, taste, and appearance **(Fantini et al., 2020).**

2.2.2 Solubility study

To perform a solubility study of Crisaborole in different solvents by visual inspection, small, equal amounts of the drug are added to test tubes containing various polar (e.g., water, ethanol) and non- polar (e.g., chloroform) solvents. The mixtures are stirred or shaken at room temperature for a fixed time, typically 15–30 minutes. After settling, the solutions are visually inspected for clarity or undissolved particles. A clear solution indicates good solubility, while cloudiness or sediment suggests poor solubility. This simple method gives a quick, qualitative idea of the drug's solubility behavior in different solvent types **(Ansari et al., 2022).**

2.2.3 pH determination

To determine the pH of Crisaborole using a digital pH meter. This helps assess the drug's acidity or alkalinity, which is important for formulation stability and compatibility **(Awan et al., 2022).**

2.2.4 Melting Point determination

To determine the melting point of Crisaborole using a melting point apparatus. Clean the apparatus after use to avoid contamination. **(Chaudhary, 2020).**

2.2.5 Determination of Lambda max and calibration curve of Crisaborole

- **Lambda (λ) max**

A stock standard solution of Crisaborole was prepared at a concentration of 1 mg/mL using 80% methanol as the solvent. From this stock, a working standard solution with a concentration of 100 µg/mL was obtained by diluting it appropriately with the same 80% methanol. The working solution was then analyzed using a Shimadzu 1700 double beam UV spectrophotometer, scanning across the wavelength range of 200 to 400 nm to obtain the UV absorption spectrum of Crisaborole **(Awan et al., 2022).**

- **Standard calibration curve**

A 100 mg quantity of Crisaborole was accurately weighed and transferred into a 100 mL volumetric flask. It was dissolved using 80% methanol, and the volume was made up to the mark with the same solvent. From this solution, 1 mL was pipetted into a 10 mL volumetric flask, diluted with methanol, and labelled as the stock solution. This stock solution was then scanned using a UV spectrophotometer over the wavelength range of

International Journal of Pharmaceutical Research and Applications
Volume 10, Issue 4 July-Aug 2025, pp: 934-948 www.ijprajournal.com ISSN: 2456-4494

200 to 400 nm to determine the maximum absorption wavelength (λ max) of Crisaborole.

2.2.6 Preparation of calibration curve

The working standard solution (100 µg/mL) was diluted to 2, 4, 6, 8, 10, and 12 µg/mL. After accurately transferring the Crisaborole working standard stock solution to a series of 5 mL calibrated flasks, the volume was adjusted using methanol. At Crisaborole 250 nm, the absorbance of the resultant solutions was measured in comparison to distilled water blank. A calibration curve was created by graphing the drug's absorbance vs concentration. A six-point calibration curve was produced for Crisaborole values ranging from 2 to 12 µg/mL **(Singh and Vingkar, 2008).**

2.2.7 Fourier transmission Infra-Red Spectroscopy

Fourier Transform Infrared (FTIR) spectroscopy is used in academic laboratories and the pharmaceutical industry to determine the structure of individual molecules and the composition of molecular mixtures. FTIR spectroscopy studied a material using modulated mid-infrared energy. Infrared light is absorbed at certain frequencies that correspond perfectly to the vibrational frequency of the molecule's atoms. When the bond energy of the vibration equals that of the mid- infrared light, the bond can absorb it. A molecule's many bonds vibrate at different energies, allowing it to absorb IR light at various wavelengths. Liposomes' FTIR spectra were collected using the KBr press pellet technique and scanned from 400 to 4000 cm−1. The KBr disc was created by mixing 1 mg of Crisaborole with 100 mg of spectroscopic grade KBr and drying under an infrared light source. To form a disc, KBr and drug were mixed and squeezed under hydraulic pressure. This disc was placed into an FT-IR chamber **(Lakshminarayanan and Balakrishnan 2020).**

2.3 Formulation and Optimization of microcapsule Containing Crisaborole

Microcapsules were prepared by solvent evaporation method. Accurately weighted Eudragit L- 100 and RS-100 in different ratios were dissolved in 20ml of acetone to form a homogenous polymers solution. Core material, i.e., Drug was dispersed in it and mixed thoroughly (Table 1). This organic phase was slowly poured at 15°C into liquid paraffin (50.0 ml) containing 1% (w/w) of Span-80 with stirring at 1000 rpm to form a uniform emulsion. The microcapsules were collected by decantation and the product was washed four times and dried at room temperature for 3 hrs. The microcapsules were then stored in a desiccator over fused calcium chloride.

Table 1: Composition of Microcapsules Formulation

Formulation	Eudragit L-100 (mg)	Eudragit RS-100 (mg)	Drug (mg)	liquid paraffin	Span-80 (%)	Acetone (ml)	Stirring Time(min.)
MF 1	250	100	200	50.0	1.0	20.0	2.5
MF 2	250	200	200	50.0	1.0	20.0	4
MF 3	50	200	200	50.0	1.0	20.0	1
MF 4	250	200	200	50.0	1.0	20.0	1
MF 5	150	300	200	50.0	1.0	20.0	4
MF 6	250	300	200	50.0	1.0	20.0	2.5
MF 7	150	200	200	50.0	1.0	20.0	2.5
MF 8	50	200	200	50.0	1.0	20.0	4
MF 9	150	100	200	50.0	1.0	20.0	4
MF 10	150	100	200	50.0	1.0	20.0	1
MF 11	150	300	200	50.0	1.0	20.0	1
MF 12	50	300	200	50.0	1.0	20.0	2.5
MF 13	50	100	200	50.0	1.0	20.0	2.5

International Journal of Pharmaceutical Research and Applications
Volume 10, Issue 4 July-Aug 2025, pp: 934-948 www.ijprajournal.com ISSN: 2456-4494

Table 2: Dependent and independent variables for optimization of formulation

Coding	Independent
X1	A: Eudragit L 100 (mg)
X2	B: Eudragit RS 100 (mg)
X3	C: Stirring time (hrs)
Dependent	
Y1	Particle size (nm)
Y2	Entrapment efficiency (%)

2.4 Evaluation parameter of Crisaborole loaded microcapsule formulation

2.4.1 Physical appearance:- The physical appearance of Crisaborole-loaded microcapsule can be evaluated by visual inspection for clarity, color, and homogeneity **(Zilles et al., 2022).**

2.4.2 Particle Size:- To evaluate the particle size of Crisaborole-loaded microcapsules, a sample is diluted appropriately with deionized water to avoid multiple scattering and then analyzed using a Malvern Zetasizer (Malvern Instruments) **(Aledresi et al., 2020).**

2.4.3 Zeta Potential:- Zeta potential of Crisaborole-loaded microcapsules is measured using the Malvern Zeta sizer by diluting the microcapsules suspension in a suitable electrolyte solution to ensure conductivity **(Andrade et al., 2018).**

2.4.4 Scanning Electron Microscopic (SEM):- The morphological properties of Crisaborole-loaded microcapsules were analyzed using a scanning electron microscope (SEM). Before imaging, the microcapsules were coated with a thin metal layer (typically 2–20 nm) such as gold, palladium, or platinum using a sputter coater under vacuum to enhance conductivity. When the electron beam of the SEM interacts with the metal-coated sample, it generates secondary electrons, including Auger electrons, which help reveal surface features. Based on principles like Rutherford and Kramer's Law, only electrons emitted at a 90-degree angle from the interaction point were selected to produce clear images of the surface topography **(Anwer et al., 2019).**

2.4.5 Entrapment efficiency

To determine the entrapment efficiency of Crisaborole-loaded microcapsules, 10 mL of the microcapsule's formulation was mixed with 5 mL of methanol in a volumetric flask. The mixture was vortexed for one minute to ensure complete drug extraction. After adjusting the final volume to 10 mL, the solution was filtered and appropriately diluted. The amount of Crisaborole entrapped in the microcapsules was then quantified using spectrophotometry **(Swetha et al., 2011).**

%EE = Initial amount of drug added - Drug amount in supernatant / Initial amount of drug added × 100

2.4.6 In-vitro drug release study

The in-vitro drug release study of crisaborole loaded microcapsules formulations were studied by dialysis bag diffusion method. Drug loaded microcapsules (5 ml) were dispersed into dialysis bag and the dialysis bag was then kept in a beaker containing 100 ml of pH 7.4 phosphate buffer. The beaker was placed over a magnetic stirrer and the temperature of the assembly was maintained at 37 ± 1 °C throughout the experiment. During the experiment rpm was maintained at 100 rpm. Samples (2 ml) were withdrawn at a definite time intervals and replaced with equal amounts of fresh pH 7.4 phosphate buffers. After suitable dilutions the samples were analyzed using UV–Visible spectrophotometer at 250 nm **(Bohrey et al., 2016).**

III. RESULT AND DISCUSSION

3.1 Pre-formulation study of Crisaborole

3.1.1 Organoleptic evaluation

The drug sample was analyzed physical appearance and the parameter

International Journal of Pharmaceutical Research and Applications
Volume 10, Issue 4 July-Aug 2025, pp: 934-948 www.ijprajournal.com ISSN: 2456-4494

Table 3: Organoleptic evaluation of Crisaborole

Physical parameter	Observation
Color	White to pale yellow
Odor	Slight in odor
State	Solid
Appearance	Crystalline powder

3.1.2 Solubility study

Table 4: Solubility study of Crisaborole

Drug	Solvents	Observation/Inference
Crisaborole	Water	Insoluble
	Ethanol	Soluble
	Methanol	Freely Soluble
	Acetone	Soluble
	DMSO	Sparingly Soluble

3.1.3 Melting Point and pH determination

Table 5: Melting Point, pH and Lambda max of Crisaborole

Drugs	Melting point	pH	Lambda max
Crisaborole	131 °C	5.3	250.0nm

3.1.5 Standard calibration curve

Table 6: Calibration Curve of Crisaborole in Methanol

Concentration (µg/ml)	Mean Absorbance
2	0.179
4	0.354
6	0.549
8	0.711
10	0.886
12	0.999
Mean	0.631
SD	0.313899
%RSD	49.746

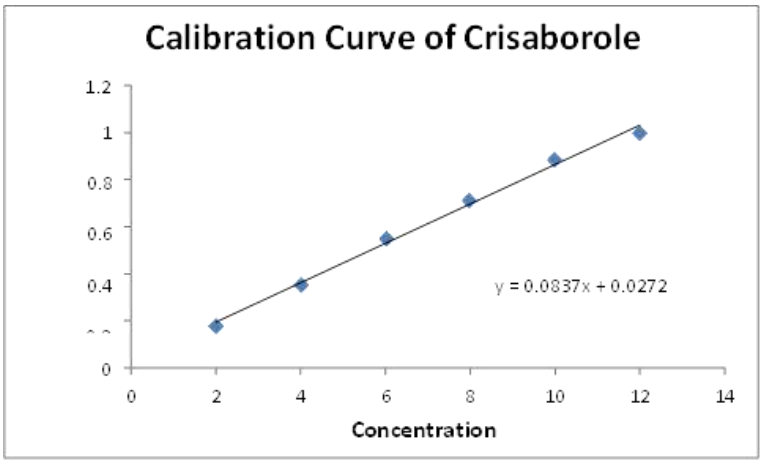

Graph 2: Calibration curve of Crisaborole

International Journal of Pharmaceutical Research and Applications
Volume 10, Issue 4 July-Aug 2025, pp: 934-948 www.ijprajournal.com ISSN: 2456-4494

3.1.6 Functional group identified by Infra-Red spectroscopy

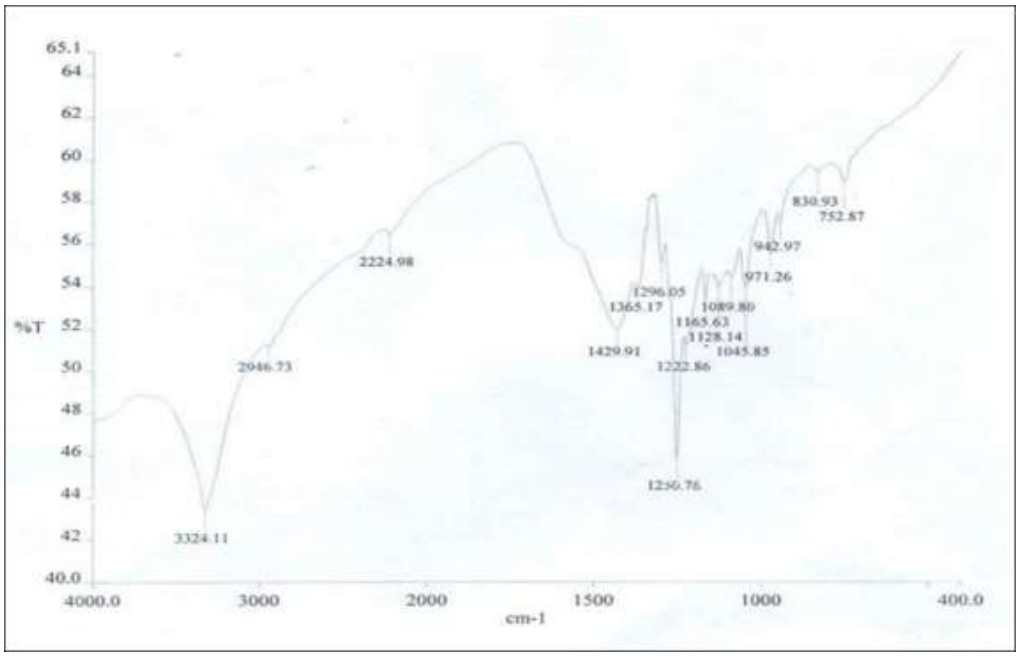

Graph 3: FTIR study of Crisaborole

Table 7: Interpretation of IR spectrum of Crisaborole

Peak obtained	Reference peak	Functional group	Name of functional group
3324.11	3550 – 3200	O-H stretch	Alcohols**
2946.73	2990 – 2850	C-H stretch	Alkanes
2224.98	2280 – 2200	C=N stretch	Nitriles
1429. 91	1440-1395	O-H bending	Carboxylic acid
1365.17	1400-1300	NO2 stretch	Nitro group
1296.71	1310-1250	C-O stretching	Aromatic ester
1128.14	1150-1085	C-O stretching	Aliphatic ether
1045.85	1050-1040	CO-O-CO stretching	Anhydride
942.97	950–910	O–H bend	Carboxylic acids
752.87	850–550	C–Cl stretch	Alkyl halides

3.2 Optimization process by Design of experiment approach

Table 8: Build Information

File Version	12.0.1.0		
Study Type	Response Surface	**Subtype**	Randomized
Design Type	Box-Behnken	**Runs**	13
Design Model	Quadratic	**Blocks**	No Blocks
Build Time (ms)	1.0000		

International Journal of Pharmaceutical Research and Applications
Volume 10, Issue 4 July-Aug 2025, pp: 934-948 www.ijprajournal.com ISSN: 2456-4494

3.2.2 Formulation trials as per Box–Behnken design

Table 10: Formulation trials

Formulation	Eudragit L-100 (mg)	Eudragit RS- 100 (mg)	Drug (mg)	liquid paraffin	Span-80 (%)	Acetone (ml)	Stirring Time (min.)	Particle size (nm)	Entrapment efficiency (%)
MF 1	250	100	200	50.0	1.0	20.0	2.5	562.1	73.11
MF 2	250	200	200	50.0	1.0	20.0	4	244.8	93.76
MF 3	50	200	200	50.0	1.0	20.0	1	839.4	65.23
MF 4	250	200	200	50.0	1.0	20.0	1	840.7	67.05
MF 5	150	300	200	50.0	1.0	20.0	4	194.5	91.28
MF 6	250	300	200	50.0	1.0	20.0	2.5	478	90.63
MF 7	150	200	200	50.0	1.0	20.0	2.5	523.2	84.35
MF 8	50	200	200	50.0	1.0	20.0	4	230.6	88.2
MF 9	150	100	200	50.0	1.0	20.0	4	241.9	91.77
MF 10	150	100	200	50.0	1.0	20.0	1	849.3	75.45
MF 11	150	300	200	50.0	1.0	20.0	1	801.6	84.75
MF 12	50	300	200	50.0	1.0	20.0	2.5	487.2	84.22
MF 13	50	100	200	50.0	1.0	20.0	2.5	566.3	79

3.3.3 Factors and responses of Variables (Constraints)

Table 11: Factors of variable

Factor	Name	Units	Type	Minimum	Maximum	Coded Low	Coded High	Mean	Std. Dev.
A	Eudragit L 100	mg	Numeric	50.00	250.00	-1 ↔ 50.00	+1 ↔ 250.00	150.00	81.65
B	Eudragit RS 100	mg	Numeric	100.00	300.00	-1 ↔ 100.00	+1 ↔ 300.00	200.00	81.65
C	Stirring time	Hrs	Numeric	1.0000	4.00	-1 ↔ 1.00	+1 ↔ 4.00	2.50	1.22

Table 12: Responses of variable

Response	Name	Units	Observations	Analysis	Minimum	Maximum	Mean	Std. Dev	Ratio	Transform	Model
R1	Vesicle size	nm	13	Polynomial	194.5	849.3	527.66	248.56	4.37	None	Linear
R2	Encapsulation efficiency	%	13	Polyn omial	65.23	93.76	82.22	9.51	1.44	None	Lin ear

3.3.4 Fit Summary

Table 13: Response 1: Particle size

Source	Sequential p-value	Adjusted R^2	Predicted R^2	
Linear	**< 0.0001**	**0.9973**	**0.9956**	**Suggested**
2FI	0.9754	0.9961	0.9894	
Quadratic	0.4841	0.9962		
Cubic				Aliased

International Journal of Pharmaceutical Research and Applications
Volume 10, Issue 4 July-Aug 2025, pp: 934-948 www.ijprajournal.com ISSN: 2456-4494

3.3.5 ANOVA for Linear model

Table 14: Response 1: Particle size

Source	Sum of Squares	Mean Square	F-value	p-value	
Model	7.399E+05	2.466E+05	1504.12	< 0.0001	significant
A-Eudragit L 100	0.5512	0.5512	0.0034	0.9550	
B-Eudragit RS 100	8339.86	8339.86	50.86	< 0.0001	
C-Stirring time	7.316E+05	7.316E+05	4461.50	< 0.0001	
Residual	1475.76	163.97			
Cor Total	7.414E+05				

Factor coding is **Coded**. Sum of squares is **Type III – Partial**

The **Model F-value** of 1504.12 implies the model is significant. There is only a 0.01% chance that an F-value this large could occur due to noise. **P-values** less than 0.0500 indicate model terms are significant. In this case B, C are significant model terms.

3.3.6 Final Equation in Terms of Coded Factors

Vesicle size (Y1) = 527.66 intercept +0.2625 X1 -32.29 X2 -302.40 X3.

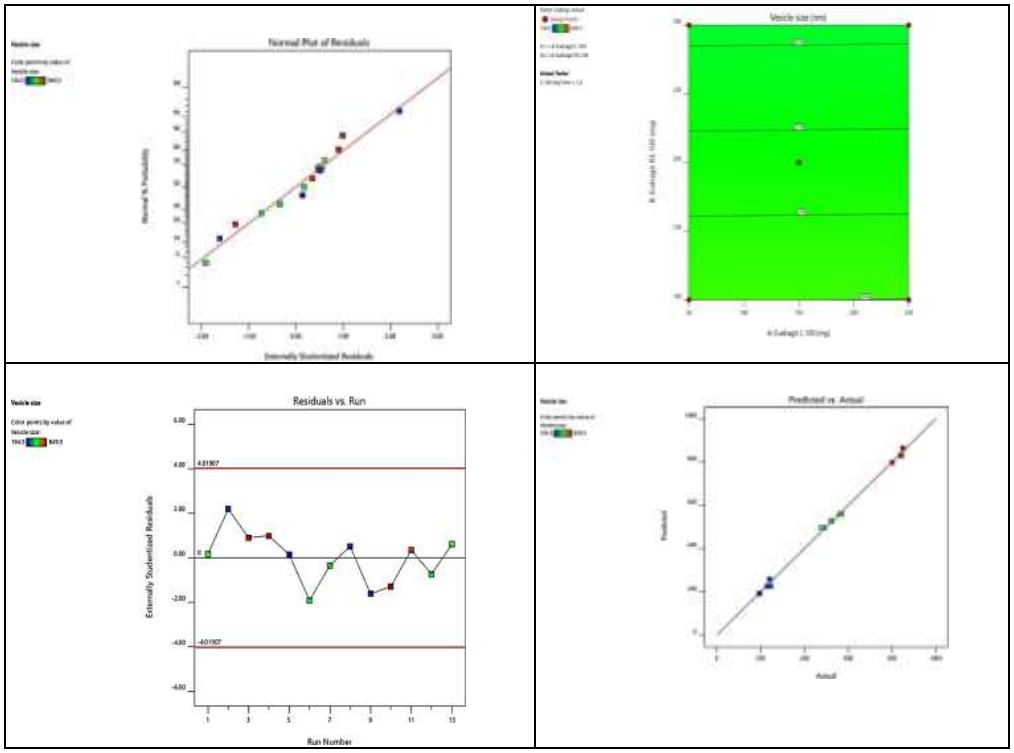

Figure 1: Two-dimensional response surface plots (normal plot vs residual, residual vs predicted and residual vs. run and Particle size) and contour plots revealing relative effects of independent variables (A: Normal plot of residuals; B: residual vs predicted and C: Residuals vs Run) on dependent variable – particle size of drug loaded microcapsules formulation

International Journal of Pharmaceutical Research and Applications
Volume 10, Issue 4 July-Aug 2025, pp: 934-948 www.ijprajournal.com ISSN: 2456-4494

3.3.7 Predicted value and observed result

Table 15: Predicted value and observed result of all formulations

Formulation code	Observed result of particle size	Predicted result of particle size	Observed result of % entrapment efficiency	Predicted result of % entrapment efficiency
PNF 1	562.10	560.21	73.11	79.26
PNF 2	244.80	225.52	93.76	92.27
PNF 3	839.40	829.80	65.23	72.16
PNF 4	840.70	830.32	67.05	74.14
PNF 5	194.50	192.97	91.28	95.23
PNF 6	478.00	495.64	90.63	87.15
PNF 7	523.20	527.66	84.35	82.22
PNF 8	230.60	225.00	88.20	90.29
PNF 9	241.90	257.55	91.77	87.34
PNF 10	849.30	862.35	75.45	69.21
PNF 11	801.60	797.77	84.75	77.09
PNF 12	487.20	495.11	84.22	85.17
PNF 13	566.30	559.69	79.00	77.28

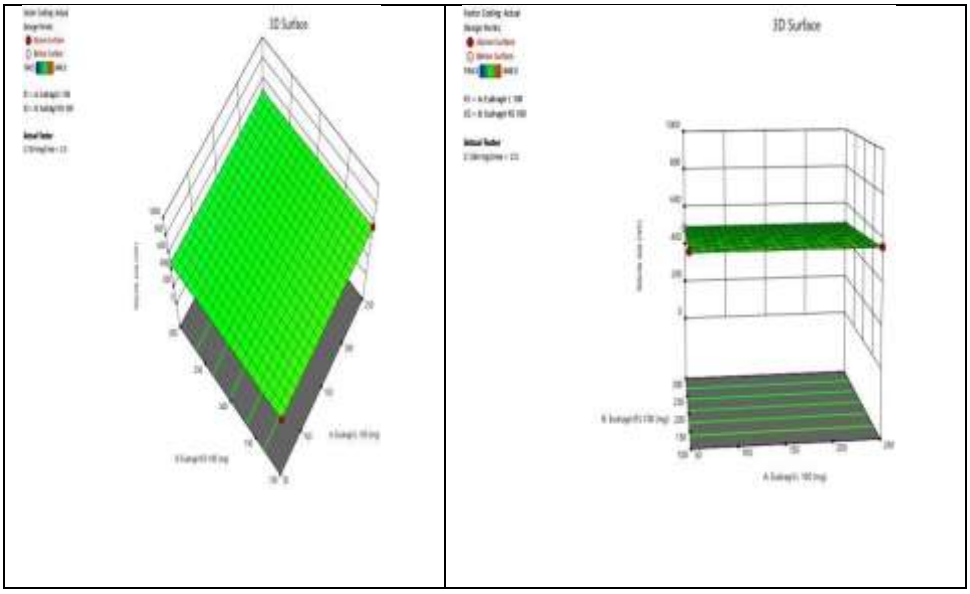

Figure 2: 3D Response surface plot showing combined effect of polymers (Eudragit RS 100 and Eudragit L 100) on particle size of microcapsule formulations

3.3.8 Effect of formulation variables on Entrapment efficiency of microcapsule formulation

Table 16: Response 2: Entrapment efficiency (Fit Summary)

Source	Sequential p-value	Adjusted R^2	Predicted R^2	
Linear	**0.0066**	**0.9765**	**0.9425**	**Suggested**
2FI	0.6574	0.5749	-0.1689	
Quadratic	0.5261	0.5575		
Cubic				Aliased

International Journal of Pharmaceutical Research and Applications
Volume 10, Issue 4 July-Aug 2025, pp: 934-948 www.ijprajournal.com ISSN: 2456-4494

3.3.9 ANOVA for linear model of Entrapment efficiency

Table 17: Response 2: Entrapment efficiency (ANOVA linear model)

Source	Sum of Squares	Mean Square	F-value	p-value	
Model	789.80	263.27	8.00	0.0066	significant
A-Eudragit L 100	7.80	7.80	0.2371	0.6379	
B-Eudragit RS 100	124.43	124.43	3.78	0.0837	
C-Stirring time	657.58	657.58	19.99	0.0016	
Residual	296.06	32.90			
Cor Total	1085.87				

Factor coding is **coded**. Sum of squares is **Type III – Partial**

The **Model F-value** of 8.00 implies the model is significant. There is only a 0.66% chance that an F-value this large could occur due to noise. **P-values** less than 0.0500 indicate model terms are significant. In this case C is a significant model term. Values greater than 0.1000 indicate the model terms are not significant. If there are many insignificant model terms (not counting those required to support hierarchy), model reduction may improve your model.

3.3.10 Final Equation in Terms of Coded Factors

Encapsulation efficiency (Y2) = +82.22 intercept +0.9875 X1 +3.94 X2 +9.07 X3.

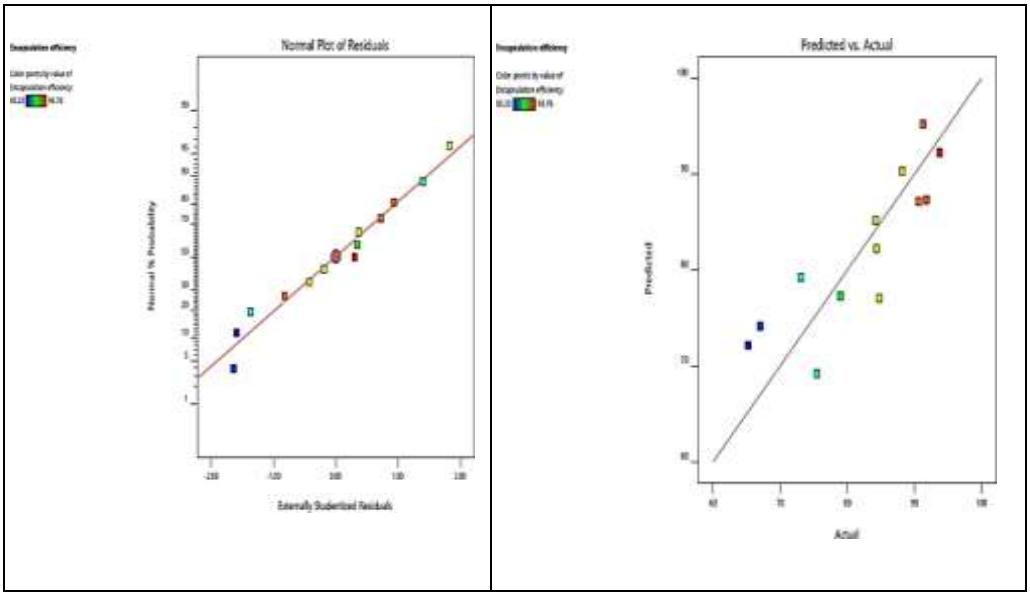

Figure 3: 2-dimensional response surface plots (Normal plot of residual, Residual vs predicted and Residual vs. Run) and contour plots revealing relative effects of independent variables (A: Eudragit L 100 concentration; B: Eudragit RS 100 concentration and C: stirring time) on dependent variable – Entrapment efficiency of drug loaded microcapsule formulation

International Journal of Pharmaceutical Research and Applications
Volume 10, Issue 4 July-Aug 2025, pp: 934-948 www.ijprajournal.com ISSN: 2456-4494

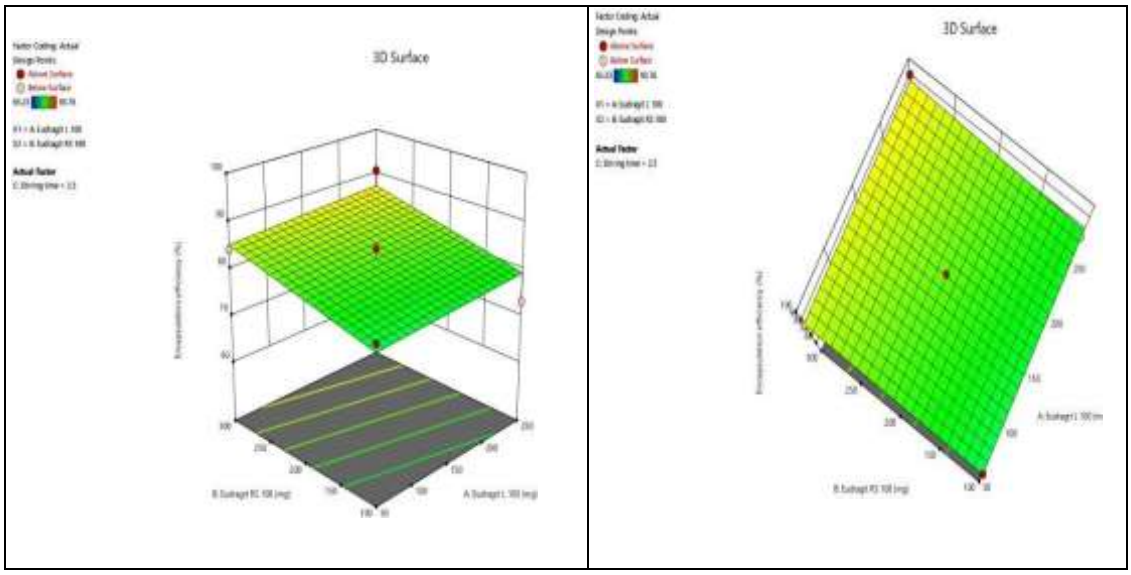

Figure 4: Response surface plot showing combined effect of polymers on Entrapment efficiency of microcapsule formulation

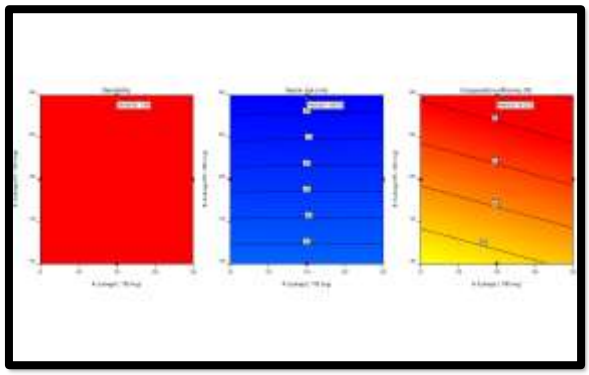

Figure5: Response surface plot showing prediction data for optimization

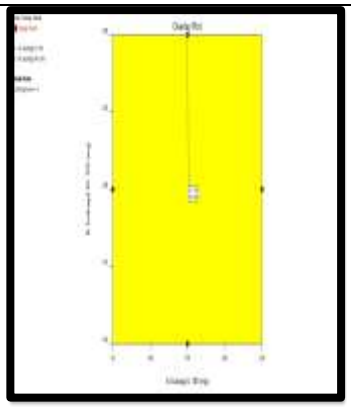

Figure 6: Overlay plot of optimization formulation

3.3.12 Optimized formula of microcapsules formulation (Point Prediction)

Table 19: Optimized formula of microcapsules formulation

Eudragit L 100	Eudragit RS 100	Stirring time	Vesicle size	Encapsulation efficiency	Desirability	
50.000	200.000	1.000	829.799	72.162	1.000	
150.000	**300.000**	**4.000**	**192.974**	**95.225**	**1.000**	**Selected**
250.000	200.000	4.000	225.524	92.269	1.000	

International Journal of Pharmaceutical Research and Applications
Volume 10, Issue 4 July-Aug 2025, pp: 934-948 www.ijprajournal.com ISSN: 2456-4494

3.4 Characterization of optimized formulation

3.4.1 Particle Size

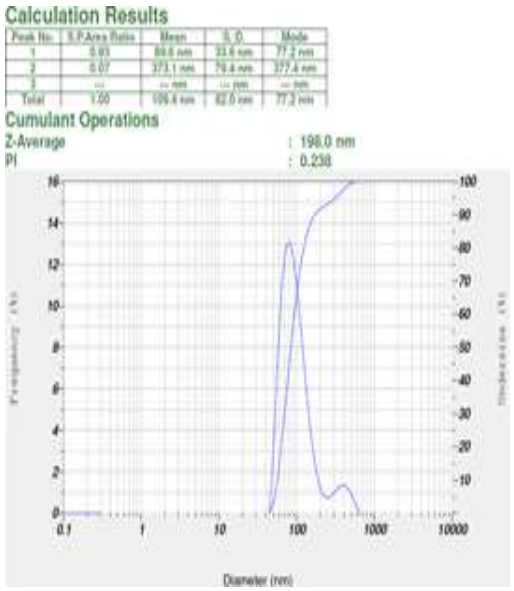

Graph 4: Particle size

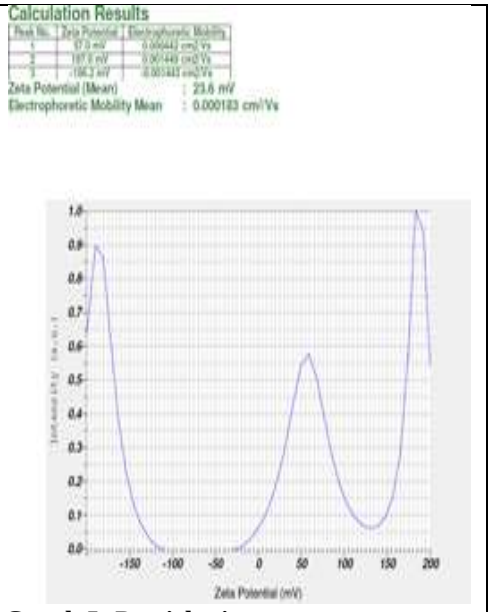

Graph 5: Particle size

Table 21: Zeta potential

Formulation	Zeta potential	Particle size (Predicted value	Particle size (Observed)
Microcapsule optimized formulation	23.6 mV	192.97 nm	198.0 nm

3.4.3 Scanning electron microscope (SEM)

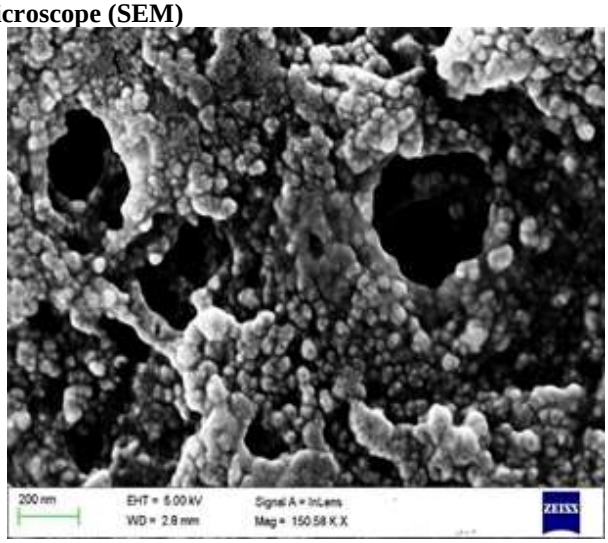

Figure 7: Microscopic analysis of the microcapsule in 150.59 KX

3.5.3 Entrapment efficacy of optimized formulation

Table 22: Entrapment efficacy

Formulations	Entrapment efficacy (Predicted value)	Entrapment efficacy (Observed result)
Microcapsules	95.**22** %	93.**78** %

International Journal of Pharmaceutical Research and Applications
Volume 10, Issue 4 July-Aug 2025, pp: 934-948 www.ijprajournal.com ISSN: 2456-4494

3.5.4 In-vitro drug release

Table 28: Release kinetics study of optimized formulation

Time (Hr)	cumulative % s drug released	% drug remaining	Square root time	log Cumu % drug remaining	log time	Log cumulative %drug released	% Drug released
0	0	100	0.000	2.000	0.000	0.000	100
1	23.11	76.89	1.000	1.886	0.000	1.364	23.11
2	36.1	63.9	1.414	1.806	0.301	1.558	12.99
4	43.13	56.87	2.000	1.755	0.602	1.635	7.03
6	57.59	42.41	2.449	1.627	0.778	1.760	14.46
8	66.83	33.17	2.828	1.521	0.903	1.825	9.24
10	77.17	22.83	3.162	1.359	1.000	1.887	10.34
12	82.41	17.59	3.464	1.245	1.079	1.916	5.24
13	97.14	2.86	3.606	0.456	1.114	1.987	14.73

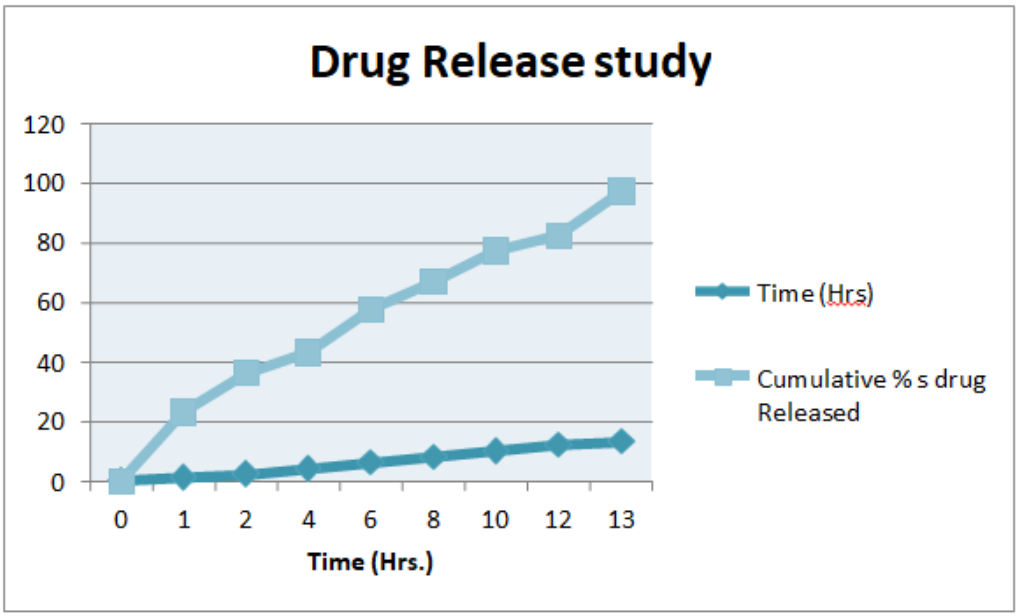

Graph 6: Release kinetics study of optimized formulation

3.6 Correlation value

Table 23: Correlation value (R^2 value)

Formulation	Model	Kinetic parameter values
Microcapsules (optimized formulation)	Zero Order	R2 = 0.9795
	First Order	R^2 = 0.8126
	Higuchi	R^2 = 0.9688
	Korsmeyerpeppas	R^2 = 0.8104

International Journal of Pharmaceutical Research and Applications
Volume 10, Issue 4 July-Aug 2025, pp: 934-948 www.ijprajournal.com ISSN: 2456-4494

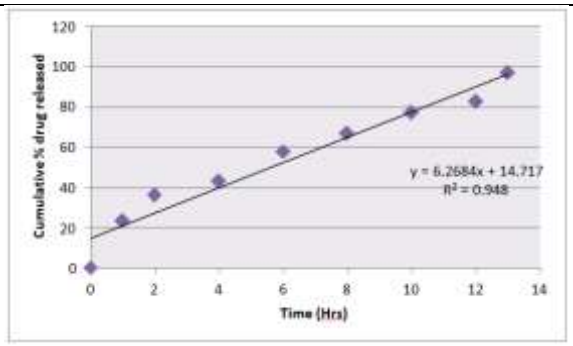

Figure 20: Zero order kinetic model

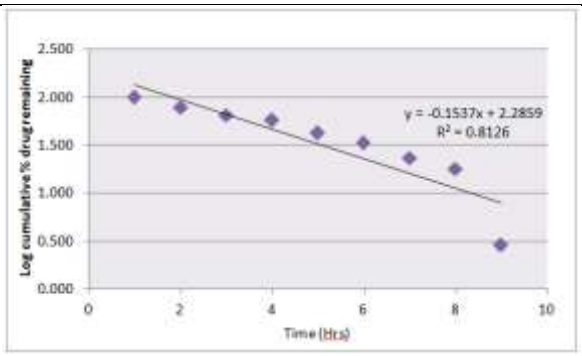

Figure 21: First Order kinetic model

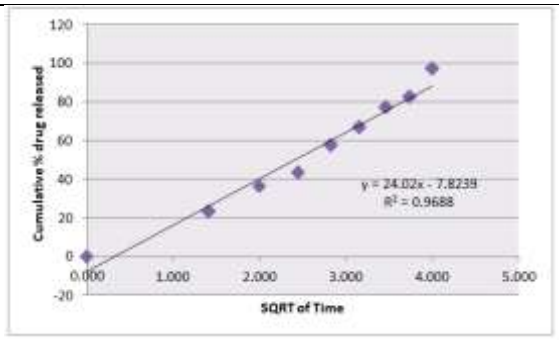

Figure 22: Higuchi model

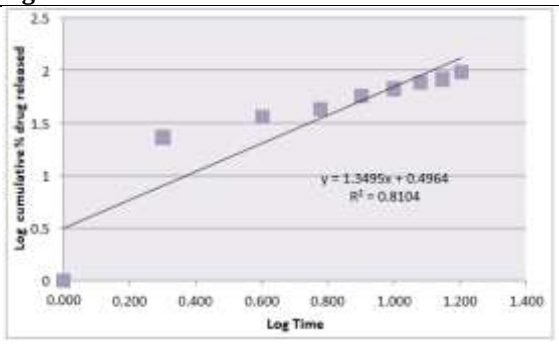

Figure 23: Korsmeyer peppas

IV. CONCLUSION

In conclusion, the application of DOE in Microcapsules formulation allows for a systematic and efficient approach to developing optimized nanocarriers for various applications. By understanding the influence of different formulation parameters, researchers can create Microcapsules with tailored properties that meet specific needs. Overall, the results validate Crisaborole's potential as a candidate for stable, effective topical formulations and as a drug encapsulated in polymeric Microcapsules to improve its solubility and therapeutic efficacy. These findings lay a strong foundation for further formulation development and clinical evaluation.

REFERENCES

[1]. Deshmukh, R., Wagh, P., & Naik, J. (2016). Solvent evaporation and spray drying technique for micro-and nanospheres/particles preparation: A review. Drying technology, 34(15), 1758-1772.

[2]. Subedi, G., Shrestha, A. K., & Shakya, S. (2016). Study of effect of different factors in formulation of micro and nanospheres with solvent evaporation technique. Open Pharmaceutical Sciences Journal, 3(1).

[3]. islam Barbhuiya, S., Shabana, K. M., & Kumar, V. (2023). Advancements in Sustained-Release Drug Delivery Systems.

[4]. Natarajan, J. V., Nugraha, C., Ng, X. W., & Venkatraman, S. (2014). Sustained-release from nanocarriers: a review. Journal of Controlled Release, 193, 122-138.

[5]. Li, H., Zuo, J., & Tang, W. (2018). Phosphodiesterase-4 inhibitors for the treatment of inflammatory diseases. Frontiers in pharmacology, 9, 1048.

[6]. McDowell, L., & Olin, B. (2019). Crisaborole: a novel nonsteroidal topical treatment for atopic dermatitis. Journal of Pharmacy Technology, 35(4), 172-178.

[7]. Vilegave, K., Vidyasagar, G., & Chandankar, P. (2013). Preformulation studies of pharmaceutical new drug molecule and products: An Overview. The American Journal of Pharmacy, 1(3), 1-20.

[8]. Fantini, A., Demurtas, A., Nicoli, S., Padula, C., Pescina, S., & Santi, P. (2020). In vitro skin retention of crisaborole after

International Journal of Pharmaceutical Research and Applications
Volume 10, Issue 4 July-Aug 2025, pp: 934-948 www.ijprajournal.com ISSN: 2456-4494

topical application. Pharmaceutics, 12(6), 491.

[9]. Ansari, M. N., Soliman, G. A., Rehman, N. U., & Anwer, M. K. (2022). Crisaborole loaded nanoemulsion based chitosan gel: formulation, physicochemical characterization and wound healing studies. Gels, 8(5), 318.

[10]. Awan, Z. A., Shoaib, A., Iftikhar, M. S., Jan, B. L., & Ahmad, P. (2022). Combining biocontrol agent with plant nutrients for integrated control of tomato early blight through the modulation of physio-chemical attributes and key antioxidants. Frontiers in microbiology, 13, 807699.

[11]. Singh, K. K., & Vingkar, S. K. (2008). Formulation, antimalarial activity and biodistribution of oral lipid nanoemulsion of primaquine. International Journal of Pharmaceutics, 347(1-2), 136-143.

[12]. Lakshminarayanan, K., & Balakrishnan, V. (2020). Screening of anti-cancer properties of Crisaborole and its derivatives against microtubules: molecular modeling approach. International Journal of Pharmaceutical and Phytopharmacological Research, 10(1), 8-21.

[13]. Zilles, J. C., Dos Santos, F. L., Kulkamp-Guerreiro, I. C., & Contri, R. V. (2022). Biological activities and safety data of kojic acid and its derivatives: A review. Experimental dermatology, 31(10), 1500-1521.

[14]. Andrade, J. G., Verma, A., Mitchell, L. B., Parkash, R., Leblanc, K., Atzema, C., ... & CCS Atrial Fibrillation Guidelines Committee. (2018). 2018 focused update of the Canadian Cardiovascular Society guidelines for the management of atrial fibrillation. Canadian Journal of Cardiology, 34(11), 1371-1392.

[15]. Anwer, M. K., Mohammad, M., Ezzeldin, E., Fatima, F., Alalaiwe, A., & Iqbal, M. (2019). Preparation of sustained release apremilast-loaded PLGA nanoparticles: In vitro characterization and in vivo pharmacokinetic study in rats. International journal of nanomedicine, 14, 1587.

[16]. Swetha, A., Rao, M. G., Ramana, K. V., Basha, B. N., & Reddy, V. K. (2011). Formulation and in-vitro evaluation of etodolac entrapped in microsponge based drug delivery system. International Journal of Pharmacy, 1(2), 73-80.

[17]. Bohrey, S., Chourasiya, V., & Pandey, A. (2016). Polymeric nanoparticles containing diazepam: preparation, optimization, characterization, in-vitro drug release and release kinetic study. Nano Convergence, 3(1)